Research article

Transcriptome profiling of barnyard millet (*Echinochloa frumentacea* L.) during grain development to reveal the genomic insights into iron accumulation

Shital M. Padhiyar, Jasminkumar Kheni, Shraddha B. Bhatt, Hiral Desai, Rukam S. Tomar [*]

Department of Biotechnology, Junagadh Agricultural University, Junagadh, 362001, Gujarat, India

ABSTRACT

In the realm of food nutritional security, the development of mineral-rich grains assumes a pivotal role in combating malnutrition. Within the scope of the current investigation, we endeavoured to discern the transcripts accountable for the improved accumulation of grain-Fe within Indian barnyard millet. This pursuit entailed transcriptome sequencing of genotypes BAR-1433 (with high Fe content) and BAR-1423 (with low Fe content) during two distinct stages of spike development—spike emergence and milking stage. In the context of spike emergence, we identified a cohort of 895 up-regulated transcripts and 126 down-regulated transcripts that delineated the difference between the high and low grain-Fe genotypes. In contrast, during the milking stage, the tally of up-regulated transcripts reached 436, while down-regulated transcripts numbered 285. The transcripts that consistently ascended in both developmental stages underwent functional annotation, aligning their roles with nucleolar proteins, metal-nicotianamine transporters, ribonucleoprotein complexes, vinorine synthases, cellulose synthases, auxin response factors, embryogenesis abundant proteins, cytochrome *c* oxidases, and zinc finger BED domain-containing proteins. Meanwhile, a heterogeneous spectrum of transcripts exhibited differential expression and upregulation throughout the distinct stages. These transcripts encompassed various facets, such as ABC Transporter family proteins, Calcium-dependent kinase family, Ferritin, Metal ion binding, Iron-sulfur cluster binding, Cytochrome family, Zinc finger transcription factor family, Ferredoxin–NADP reductase type 1 family, Putative laccase, Multicopper oxidase family, and Terpene synthase family. To authenticate the reliability of these transcripts, six contigs representing probable functions, including metal transporters, iron sulfur coordination, metal ion binding, auxin-responsive GH3-like protein 2, and cytochrome P450 71B16, were harnessed for primer design. Subsequently, these primers were utilized in the validation process through qRT-PCR, with the outcomes aligning harmoniously with the transcriptome results. This study chronicles a constellation of genes linked to elevated iron content within barnyard millet, showcasing a proof of concept for leveraging transcriptome insights in marker-assisted selection to fortify barnyard millet with iron. This marks the inaugural comprehensive transcriptome analysis delineating transcripts associated with varying levels of grain-iron content during the panicle developmental stages within the barnyard millet paradigm.

* Corresponding author.
  E-mail address: rukam@jau.in (R.S. Tomar).

1. Introduction

Barnyard millet, a member of the Poaceae family, subfamily Panicoideae, and tribe Paniceae, comprises two distinct cultivated species: *Echinochloa utilis* and *Echniochloa frumentacea*. The former, known as Japanese barnyard millet, contrasts with the latter, *E. frumentacea*, which is referred to by various names including sawa millet, billion-dollar grass, and Indian barnyard millet [1]. As the fourth most produced minor millet, barnyard millet contributes significantly to global food security, especially for impoverished populations. This minor cereal holds cultivation prominence across diverse regions, including India, China, Japan, Pakistan, Nepal, and African countries which include Niger, Nigeria, Sudan, Mali, Ethiopia, Senegal, Burkina Faso, etc [2]. Over the last three years, India has emerged as the principal barnyard millet producer, boasting a yield of 0.147 million tonnes and the largest cultivated area, spanning 0.146 million hectares, with an average productivity of 1034 kg/ha [3].

Originating from warm and temperate climes worldwide, barnyard millet, specifically the *Echinochloa* species, stands as an ancient cereal crop. With multifaceted utility, this crop serves both as a staple food and a fodder source. Renowned for its resilience in the face of drought, rapid growth, and adaptability to diverse environmental conditions, as well as nutrient-deprived soils [4], barnyard millet possesses exceptional agronomic qualities. Beyond these attributes, its grains possess noteworthy nutritional value and prove economically advantageous when compared with major cereals such as rice, wheat, and maize. Highlighting its significance, barnyard millet boasts substantial protein content (11.1 %), carbohydrates (65 %), dietary fiber (9.8 %), and notably essential micronutrients, including iron (Fe) and zinc (Zn), known for their manifold health benefits [5]. *E. frumentacea* notably exhibits the potential in lowering blood glucose levels, surpassing its minor millet counterparts [6]. These remarkable attributes position barnyard millet as an optimal crop for subsistence farmers, doubling as a contingency replacement during the potential failure of major crops during the kharif season.

In recent times, micronutrient deficiency has emerged as a global concern, particularly in nations that are categorized as underdeveloped and developing nations. Iron deficiency-induced anemia has become a critical public health issue, affecting 42 % of pregnant women, 30 % of non-pregnant women (aged 15 to 50), 47 % of preschool children (under 5 years), and 12.7 % of young males (>15 years), according to a World Health Organization (WHO) report [7]. Iron deficiency anemia not only impairs children's growth and cognitive development but also negatively impacts the cognitive, physical, and psychological health of non-pregnant women and maternal and neonatal outcomes in pregnant women. In many Asian and African countries, the prevalence of iron deficiency anemia among women aged 15 to 49 exceeds 40 %. The consumption of milled rice, wheat, and maize, with their dense nutrient profiles, has eclipsed traditional, nutrient-rich crops in developing nations. While starch is abundant in these refined diets, they lack vital minerals, particularly micronutrients like iron and zinc. Given that the majority (>80 %) of diets in developing countries consist of low-iron staple foods, it is implausible to meet iron requirements from the remaining 20 % of the diet. Consequently, diversifying staple foods by incorporating naturally iron-rich crops like millets is crucial. Furthermore, millets offer substantially more dietary fiber (6.4–11.5 g/100g), 2.3 to 4.0 times more than refined rice and wheat, nourishing gut flora and positively impacting gut composition [8]. Indian barnyard millet stands out for its robust iron content and other micronutrients. A mere cup of 100 g of barnyard millet can provide 100 % of the daily iron requirement and 67 % during pregnancy, along with a significant calcium contribution. Numerous studies have unveiled the nutritional profile of barnyard millet, emphasizing its high iron and zinc content in the grains. However, despite this knowledge, the untapped potential of this crop remains largely unexplored, owing to the post-green revolution focus on staple crops such as rice, wheat, and maize to enhance food production. Moreover, the dearth of genomic information on barnyard millet hampers the integration of modern breeding and biotechnological approaches in crop improvement initiatives. While Expressed Sequence Tag (EST) methods have accelerated research across various crops [9], their application in barnyard millet remains scant. Consequently, the need to expedite research activities concerning this vital crop underscores the urgency to bolster its genomic and transcriptomic resources.

In recent years, the advent of next-generation sequencing (NGS) technologies has yielded remarkable insights, enriched genomic resources and unraveling pivotal molecular mechanisms governing specific biological processes. This technological stride has enabled large-scale sequencing, emerging as a potent tool with diverse applications in plant biology, including transcriptome analysis and genome sequencing [10]. RNA-Sequencing, a comprehensive transcriptome sequencing technique, facilitates precise gene expression quantification at the transcriptional level, unraveling non-coding regions, defining transcript structures, and identifying differentially expressed genes linked to essential agronomic traits [11]. Its potential extends to unraveling secondary metabolic pathways, disease-associated transcripts, and novel genes [12].

A biofortification breeding program geared towards elevating iron content in barnyard millet genotypes holds the promise of mitigating anemia and meeting daily human iron requirements. Incorporating advanced biotechnological tools into conventional breeding strategies could expedite this biofortification initiative. A thorough exploration of genes governing iron accumulation and related pathways is imperative. In this study, we present the transcriptome of high iron content Indian barnyard millet across two distinct spike development stages. By comparing samples from genotypes characterized by high and low grain-iron content, we aim to identify differentially expressed genes implicated in iron accumulation within the grains.

2. Materials and methods

2.1. Plant genotypes and Fe concentration

Genotypes of Indian barnyard millet (*Echinochloa frumentacea* L.) were procured from the ICAR-Indian Institute of Millets Research

(ICAR-IIMR), located in Rajendra Nagar, Hyderabad, Telangana, India. All necessary permissions for conducting this research were obtained, and the entire study was conducted in adherence to the institute's prescribed guidelines for working with this plant species. The entire process, from seed collection to experimentation, was conducted in accordance with both national and institutional guidelines, ensuring compliance with international standards as well. Specifically, seeds from 30 distinct genotypes were sown in a multiplication plot within the Department of Biotechnology during the Kharif season of 2020, precisely in the second fortnight of June. The experiment was conducted in three replications using a Randomized Complete Block Design (RCBD) to ensure robust results. Upon maturation, individual seeds were harvested and subjected to Fe (iron) content analysis. This analysis was carried out in triplicate, utilizing the wet oxidation method, with subsequent digestion using a diacid mixture of HNO_3 and $HClO_4$ in a 3:1 ratio. Measurement of Fe content was accomplished using microwave plasma atomic emission spectroscopy (MP-AES) from Agilent Technologies. The specific parameters employed included an emission wavelength of 259.94 nm, a viewing position set at zero, and a nebulizer gas flow rate of 0.6 L/min.

Among the thirty genotypes studied, one genotype, labelled as BAR-1433, exhibited notably high Fe content. In contrast, another genotype, BAR-1423, demonstrated low Fe content and was designated as the control for subsequent comparisons. Following these preliminary assessments, genotypes BAR-1433 and BAR-1423 were then cultivated under field conditions, adhering to recommended agricultural practices. These practices encompassed the application of NPK (nitrogen, phosphorus, and potassium) in a 40:20:0 ratio, with nitrogen being applied in two separate doses of 20 kg each as recommended by ICAR-IIMR.

For transcriptomic analysis, samples were collected from both genotypes at two distinct stages: spike emergence and milking stage as maximum activity related to Fe accumulation takes place during these stages [13]. The time points for collection were 35 days after sowing (DAS) and 55 DAS, respectively, with each stage being replicated three times. To preserve the integrity of the samples, they were promptly frozen using liquid nitrogen and subsequently stored at a temperature of −80 °C until the RNA extraction process was initiated.

2.2. RNA extraction and high-throughput sequencing

Total RNA extraction was carried out from a total of 12 samples, encompassing three replicates each from two distinct genotypes at two different developmental stages. The TRIzol Reagent (Invitrogen, based in Carlsbad, California, United States) was initially utilized for this purpose. Subsequently, the RNeasy Plant Mini Kit, manufactured by QiaGen located in Valencia, CA, was employed according to the manufacturer's protocol. To ascertain the quality of the extracted RNA, 1.0 % agarose gel electrophoresis was performed. Additionally, the concentration of the RNA samples was quantified using the Qubit® RNA HS Assay Kit from Invitrogen[TM], along with the Qubit® 2.0 Fluorometer[TM].

For the isolation of mRNA, approximately 1 μg of the total RNA was utilized, following the protocols outlined in the Dynabeads® mRNA DIRECT™ Kit (Thermofisher Scientific, USA). After the purification process, the mRNA underwent fragmentation through the use of the RNase enzyme. This enzymatic action occurred at a temperature of 37 °C within the provided RNAase buffer. The cDNA library preparation was executed using the Total RNA-Seq Kit v2 (Thermofisher Scientific, USA). To generate fragments suitable for reverse transcription, random hexamers and Superscript II reverse transcriptase from Invitrogen[TM] were employed. Subsequently, a PCR amplification step was conducted on the cDNA library to enrich the adapter-ligated fragments. Notably, individual samples were molecularly barcoded during this library preparation stage, facilitating their differentiation during subsequent downstream analysis. The quality and quantity of each resulting library were assessed. Measurements were conducted using the Qubit 2.0 Fluorometer, and validation was performed through the use of E-Gel 2 % Agarose, a product from Invitrogen[TM]. Following these preparation steps, the libraries for each sample were diluted to a concentration of 100pM. These libraries were then subjected to emulsion PCR utilizing the Ion OneTouch[TM] 2 system from Thermofisher Scientific in the USA. Subsequently, the enriched templates were subjected to sequencing using the ION S5[TM] system, also from Thermofisher Scientific.

2.3. Pre-processing of RNA-Seq data and de novo assembly

The initial step involved the removal of low-quality reads from the individual sequence data files of each sample. Reads containing more than 50 % bases with low-quality scores and/or over 10 % bases classified as unknown (N bases) were eliminated from the raw data. This was done to ensure result accuracy. The software tools CLC Genomics Workbench 20.0 [14] and Prinseq quality control tools (http://prinseq.sourceforge.net/) were utilized for this purpose. Following the initial quality filtering, further processing was conducted to remove adapters and low-quality sequences (those with a quality score below Q30) from the raw reads. This step was carried out using CLC Genomics Workbench 20.2, applying specific parameters [15]. The assessment of RNA-Seq read quality both before and after trimming was performed using FastQC [16]. For the purpose of de novo transcriptome assembly, Trinity (version 2.11.0) was employed with default settings [17,18]. In order to reduce redundancy within the assembly, CAP3 [19] was utilized. Furthermore, to achieve a reduction in transcript redundancy and generate distinct genes (referred to as "unigenes"), the CD-HIT program (version 4.8.1) was employed. Default parameters were used, including a similarity threshold of 95 % [20]. To predict the coding regions within the assembled transcripts, TransDecoder (version 5.5.0) was utilized (http://transdecoder.github.io). This step aids in identifying potential protein-coding regions within the transcripts, contributing to a deeper understanding of the genetic information contained within the data.

2.4. De novo transcriptome profiling

The replicated reads were individually aligned, and subsequently merged to create four distinct samples, which were then utilized for various analyses. The evaluation of transcript expression levels was based on the count of reads aligning to each transcript. For this purpose, CLC RNA-Seq analysis was employed to align the reads from each sample onto the previously assembled transcripts [21]. The assembler yielded annotated transcripts, complete with annotated length, coverage, RPKM (Reads Per Kilobase Million), and TPKM (Transcripts Per Kilobase Million) values for each of the samples. The outcome of the alignment process was then fed into a tool designed for differential expression analysis. This tool quantifies the abundance of a specified set of target sequences, extracted from sampled sub sequences. The quantification is carried out using a Generalized Linear Model (GLM) approach based on the negative binomial distribution [22]. The estimation of gene expression levels was conducted utilizing the RPKM metric, along with the q-value, which represents the False Discovery Rate (FDR) adjusted p-value. Specifically, genes displaying RPKM fold changes greater than 2 or less than −2, coupled with FDR-corrected p-values below 0.05, were identified as Differentially Expressed Genes (DEGs). These DEGs signify genes that exhibit statistically significant changes in expression between the analyzed groups or conditions. In essence, this analytical pipeline allows for the identification of genes whose expression levels differ notably under the experimental conditions, providing valuable insights into the molecular dynamics and potential regulatory mechanisms underlying the studied biological processes.

2.5. Functional annotation

Functional annotations were assigned to the unigenes using the Basic Local Alignment Search Tool (BLAST) and BLAST2GO. This process involved comparing the sequences against existing databases with an e-value threshold of 1E-6 [23,24]. For the purpose of pathway analysis, the Differentially Expressed Genes (DEGs) underwent annotation [25]. Gene Ontology (GO) classification and Kyoto Encyclopedia of Genes and Genomes (KEGG) pathway enrichment were performed on the up- and down-regulated genes displaying significant differences in gene proportion between the two genotypes. To further explore the enriched pathways of the DEGs, the gene IDs were input into ShinyGO 0.77 (http://bioinformatics.sdstate.edu/go/), a tool used for pathway enrichment analysis [26]. This step aids in unraveling the functional significance of the differentially expressed genes within the context of biological pathways and processes. For a comprehensive understanding of the barnyard millet transcriptome analysis workflow, refer to Supplementary Fig. 1, which provides a detailed visual representation of the sequential steps undertaken throughout the analytical process.

2.6. Validation of DEGs through qRT-PCR analysis

To validate the involvement of transcripts in iron (Fe) accumulation during various spike developmental stages, stored RNA samples were employed. Complementary DNA (cDNA) was synthesized from a portion of the total RNA using the QuantiTect Reverse Transcription Kit (QIAGEN, USA). This cDNA served as the template for conducting qRT-PCR (Quantitative Real-Time Polymerase Chain Reaction). Six contigs were specifically chosen for this validation process based on their assigned Gene Ontology (GO) terms. These contigs exhibited differential gene expression and were either associated with metal/ion transport or played a direct role in Fe-related functions. The primer sequences for these selected contigs were designed using Primer3 software, with a focus on their involvement in Fe accumulation [27]. Subsequent to primer design, qRT-PCR was carried out using the QuantiFast SYBR Green PCR Master Mix (QIAGEN, USA). The ABI-7300 Real-Time PCR detection system from Applied Biosystems was employed for this purpose. The qRT-PCR procedure involved running 40 cycles, with each cycle including a melt curve step at an average annealing temperature of 56 °C. In order to ensure accurate normalization, the elongation factor (EF1) transcript was utilized as an endogenous reference. To establish a linear relationship, PCR conditions were optimized for each set of target genes. Finally, the computation of differential gene

Table 1
Sample details and concentration of Fe in the grains of barnyard millet genotypes.

Sr No	Genotypes	Fe (mg/100g)	Sr No	Genotypes	Fe (mg/100g)	Sr No	Genotypes	Fe (mg/100g)
1	BAR-1406	5.52 ± 0.13	11	BAR-1416	5.46 ± 0.08	21	BAR-1426	6.76 ± 0.05
2	BAR-1407	6.82 ± 0.09	12	BAR-1417	5.4 ± 0.05	22	BAR-1427	4.22 ± 0.04
3	BAR-1408	7.69 ± 0.13	13	BAR-1418	5.38 ± 0.09	23	BAR-1428	5.48 ± 0.12
4	BAR-1409	5.79 ± 0.11	14	BAR-1419	4.98 ± 0.04	24	BAR-1429	10.18 ± 0.17
5	BAR-1410	5.07 ± 0.06	15	BAR-1420	5.98 ± 0.04	25	BAR-1430	5.97 ± 0.04
6	BAR-1411	6.14 ± 0.11	16	BAR-1421	8.09 ± 0.09	26	BAR-1432	4.94 ± 0.08
7	BAR-1412	6.54 ± 0.06	17	BAR-1422	4.34 ± 0.06	27	BAR-1433	13.14 ± 0.09
8	BAR-1413	6.49 ± 0.07	18	BAR-1423	3.83 ± 0.02	28	BAR-1434	8.92 ± 0.04
9	BAR-1414	5.53 ± 0.03	19	BAR-1424	4.8 ± 0.13	29	BAR-1329	5.74 ± 0.08
10	BAR-1415	5.8 ± 0.06	20	BAR-1425	4.61 ± 0.06	30	BAR-1489	5.9 ± 0.12
	Mean	6.18						
	Minimum	3.83						
	Maximum	13.14						
	S.Em.	0.050						
	C.D. at 5 %	0.142						
	C·V. %	1.405						

expression was performed in terms of ΔΔCT fold change values, adhering to the methodology outlined by Livak and Schmittgen in 2001 [28]. This approach allows for a quantitative assessment of the relative expression levels of the selected genes under different conditions, shedding light on their potential roles in Fe accumulation during spike developmental stages.

3. Results

3.1. Concertation of Fe in barnyard millet

Seeds obtained from ICAR-IIMR were planted at the Department of Biotechnology, JAU, in three separate sets to both increase the seed quantity and analyze them for their iron (Fe) content. The concentration of iron in the seeds of 30 different barnyard millet genotypes was determined using Microwave Plasma Atomic Emission Spectroscopy (MP-AES). This analysis involved using a diacid mixture of nitric acid (HNO3) and perchloric acid (HCIO4) for digestion, and the measurements were carried out in three repetitions.

The results showed significant variations in the genetic makeup of the barnyard millet genotypes with regard to their iron concentration. The range of iron content varied from 3.83 mg per 100 g (mg/100g) to 13.14 mg/100g across the 30 genotypes (Table 1). The genotype labelled as BAR-1433 displayed the highest iron content, while the genotype BAR-1423 exhibited the lowest iron content.

These two genotypes, BAR-1433 and BAR-1423, which possessed notably different iron content, were selected for transcriptome sequencing. The purpose of this sequencing was to identify genes that are expressed differently in terms of iron content. This analysis aimed to uncover genetic factors that might contribute to the observed variations in iron concentration.

3.2. RNA sequencing and denovo assembly

Transcriptome sequencing was conducted on both genotypes, BAR-1433 and BAR-1423, with three replications at two different stages of panicle development i.e. spike emergence and milking stage. Samples were collected from both genotypes during these developmental stages. The high iron-containing genotype yielded an average of 4.28 million raw reads, while the low iron-containing genotype produced 7.23 million reads (Table 2). The raw data underwent processing steps, including adaptor trimming and quality checks for base accuracy. It was determined that over 87 % of the total reads were of high quality, and these were subsequently utilized for mapping against the de novo assembly of barnyard millet. Three different assembly software namely CLC, SOAP denovo trans, and Trinity assembler were used for generating the assembly. The outcomes of these assemblies are described in Table 3, which provides a comprehensive overview of the employed assemblers and their corresponding results. In particular, the total count of transcripts, encompassing singletons, was found to be 225,035, 177,466, and 488,689 for CLC, SOAP denovo trans, and Trinity assembler, respectively. This summary provides a detailed outline of the assembly procedures and their outcomes, as outlined in Table 3.

3.3. Differential expression of transcripts

The transcripts obtained from replicated samples were pooled together for the purpose of identifying differentially expressed transcripts. In the comparison between the High Iron (HFe) and Low Iron (LFe) containing genotypes at the spike emergence stage, a group of 895 transcripts exhibited up-regulation, while 126 transcripts displayed down-regulation (Supplementary Fig. 2 and Supplementary Table S1). Moving on to the milking stage, there were 436 up-regulated and 285 down-regulated transcripts (Supplementary Fig. 3 and Supplementary Table S2). Upon combining and comparing the transcripts from both developmental stages (spike emergence and milking), a total of 957 transcripts were found to be either up-regulated or down-regulated during the spike emergence stage. Similarly, during the milking stage, 657 transcripts showed either up-regulation or down-regulation. Intriguingly, 64 transcripts demonstrated common patterns of either up-regulation or down-regulation in the High Iron genotype (HFe) (Fig. 1A). Specifically focusing on the transcripts that were up-regulated during the spike emergence and milking stages, there were 895 and 436 such transcripts respectively. Out of these, 27 transcripts were consistently up-regulated across both stages (Fig. 1B). Turning attention to

Table 2

Reads, de-novo assembly and mapping statistics of different stage of High and Low-Fe containing genotypes of barnyard millet.

Raw reads Name	Total Number of raw reads	Total number of high quality reads after quality control & Percentage trimmed (%)
HFe_Spike _R1	49,58,173	4,490,055 (90.56 %)
HFe_Spike _R2	60,36,437	4,962,450 (82.21 %)
HFe_Spike _R3	20,12,050	1,664,695 (82.74 %)
HFe_milking R1	40,81,195	3,654,762 (89.55 %)
HFe_milking R2	58,74,780	5,169,355 (87.99 %)
HFe_milking R3	27,30,263	2,416,438 (88.51 %)
LFe_Spike_R1	47,77,732	4,224,165 (88.41 %)
LFe_Spike _R2	48,44,317	4,049,722 (83.6 %)
LFe_Spike _R3	22,42,520	1,768,627 (78.87 %)
LFe_milking R1	70,91,421	6,543,373 (92.27 %)
LFe_milking R2	1,27,79,824	11,587,914 (90.67 %)
LFe_milking R3	1,16,80,499	10,824,581 (92.67 %)

Table 3
De Novo assembly statistics of master assembly.

	BM_CLC	BM_SOAP denovo_Trans	BM_TRINITY	BM_CAP3	BM_Unigenes
# contigs (>= 0 bp)	225035	177466	488689	27228	20849
# contigs (>= 1000 bp)	10288	180	94963	12544	9474
# contigs (>= 5000 bp)	14	0	652	127	111
# contigs (>= 10000 bp)	0	0	16	5	5
Total length (>= 0 bp)	99530747	31851533	340205016	31871464	24424427
Total length (>= 1000 bp)	14804104	211325	158717873	22881994	17550212
Total length (>= 5000 bp)	80262	0	3964192	775697	684999
Total length (>= 10000 bp)	0	0	177893	56199	56199
# contigs	57231	3932	237463	22277	16848
Largest contig	9642	1933	12255	12254	12254
Total length	45978422	2588014	259145907	29978933	22897258
GC (%)	46.05	46.33	46.21	46.75	46.76
N50	786	636	1202	1570	1604
N90	539	521	611	723	719
L50	19619	1614	68319	6273	4669
L90	48367	3426	190569	17344	13065
#N's per 100 kbp	0.00	0.00	0.00	0.00	0.00

the down-regulated transcripts, 22 of them were commonly down-regulated during both developmental stages (spike emergence and milking). Additionally, there were 104 transcripts that were uniquely down-regulated during the spike emergence stage, while 263 transcripts displayed unique down-regulation during the milking stage (Fig. 1C).

3.4. Functional annotation of differentially expressed transcripts

Annotation of the 64 differentially expressed transcripts, which exhibited common expression patterns during both developmental stages, by aligning them with the NR and UniProt databases. These transcripts that were consistently up-regulated across both stages were associated with various functional roles including nucleolar protein, metal-nicotianamine transporter, ribonucleoprotein complex, Vinorine synthase, Cellulose synthase, Auxin response factor, embryogenesis abundant protein, Cytochrome *c* oxidase, and Zinc finger BED domain-containing protein. Conversely, the transcripts that were down-regulated during both stages were linked to functions such as Chitinase, bZIP transcription factor, Light-independent protochlorophyllide reductase, Nitrate reductase, Phenylalanine ammonia-lyase, Lysine-specific histone demethylase, and Bifunctional pectinesterase (Supplementary Table S3). Additionally, Gene Ontology (GO)-based classification for the up- and down-regulated transcripts during both the spike emergence and milking
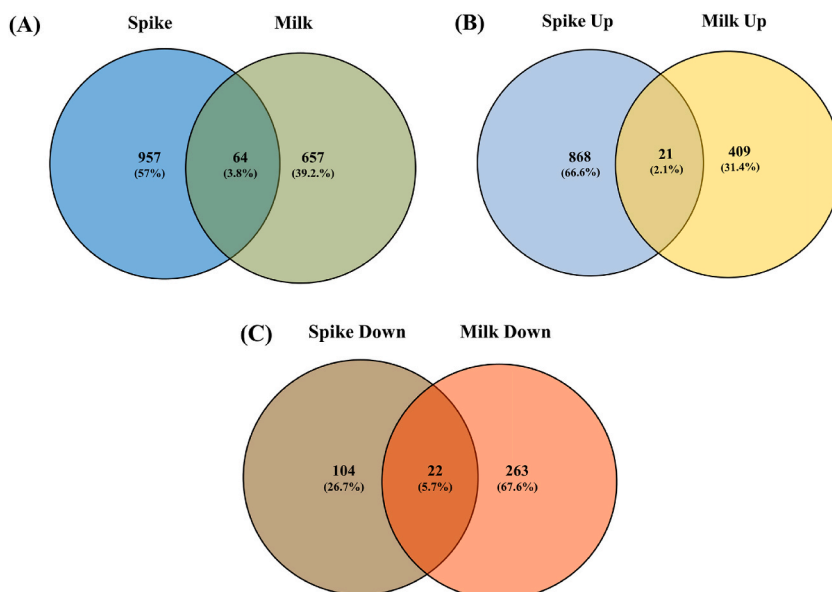

Fig. 1. Over-all distribution of Differentially Expressed Genes (DEGs) in Barnyard millet genotype (A)- Venn diagram showing the distribution of unique and common DEGs in spike and milking stages of barnyard millet; (B) - Venn diagram showing the distribution of up regulated genes in spike and milking stages of Barnyard millet; (C)- Venn diagram showing the distribution of down regulated genes in spike and milking stages of Barnyard millet.
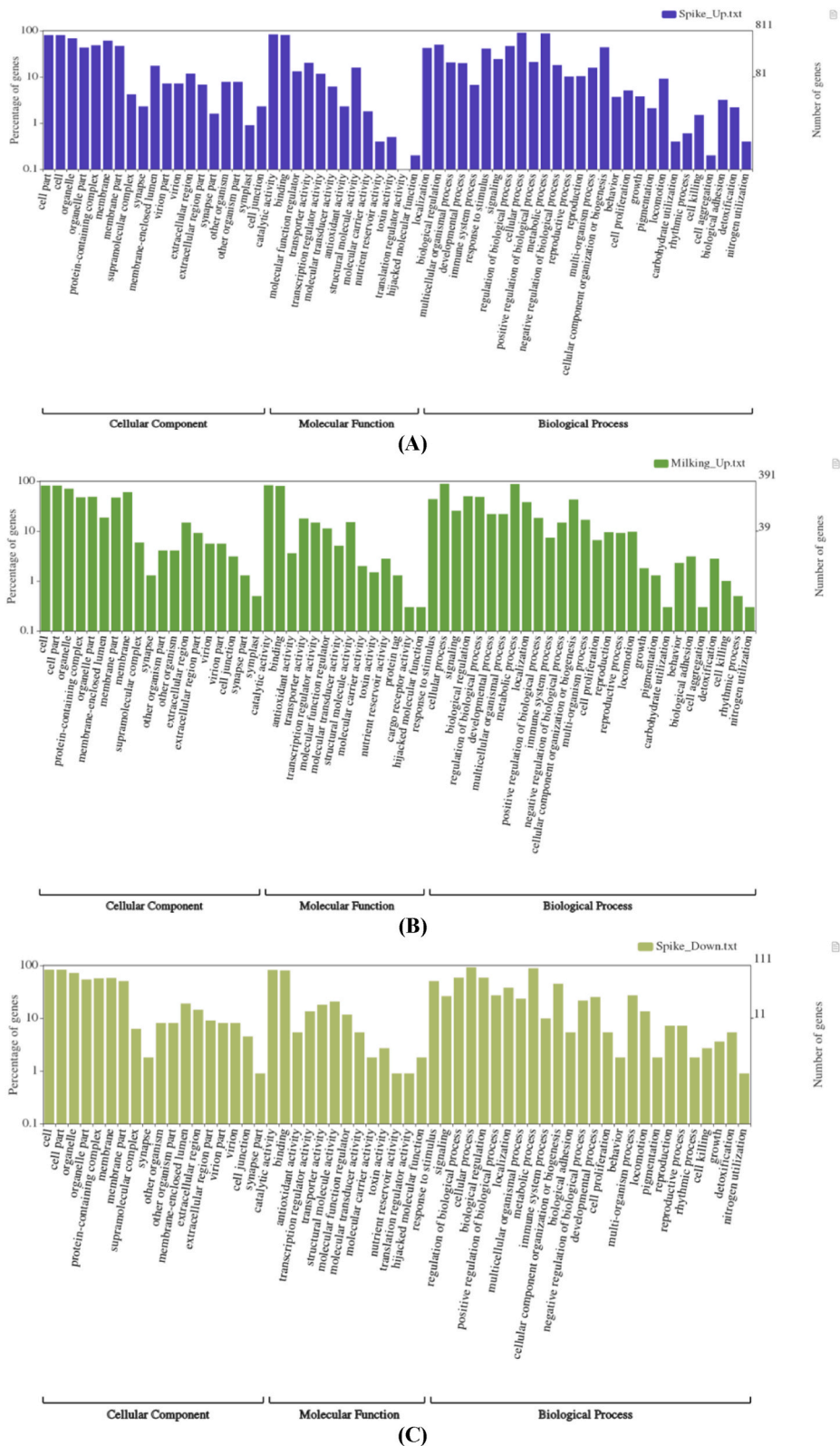
Fig. 2. (A)- GO enrichment analysis of DEGs were classified into up-regulated regulated in spike stage (cellular component, molecular function and biological process sub categories); (B)- GO enrichment analysis of DEGs were classified into up-regulated regulated in milking stage (cellular component, molecular function and biological process sub categories); (C)- GO enrichment analysis of DEGs were classified into down-regulated

regulated in spike stage (cellular component, molecular function and biological process sub categories); (D)- GO enrichment analysis of DEGs were classified into down-regulated regulated in milking stage (cellular component, molecular function and biological process sub categories).
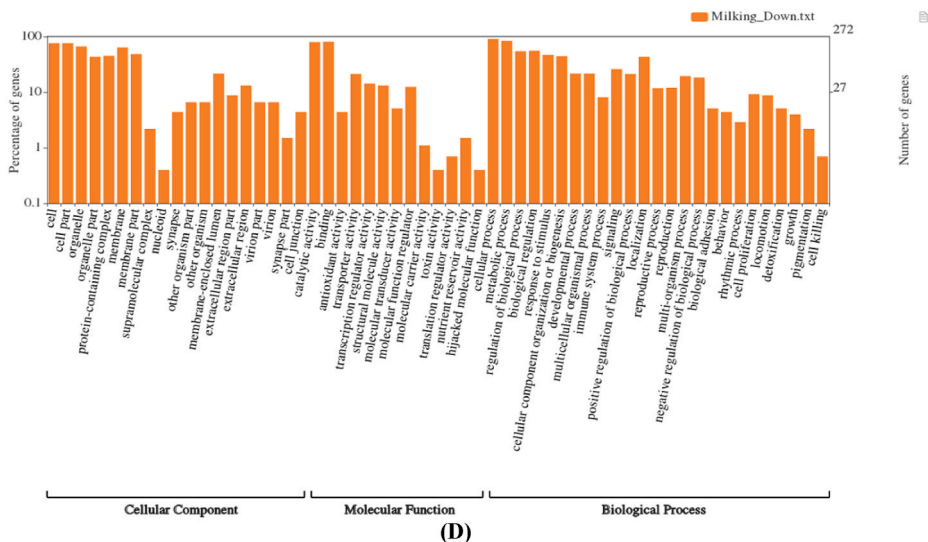

(D)

Fig. 2. (*continued*).

stages was carried out. Out of the total 895 transcripts that were up-regulated during the spike emergence stage, 811 transcripts showed significant enrichment with GO terms. In terms of Biological Process (BP) GO terms, the up-regulated transcripts were associated with functions such as biological regulation, multicellular organismal process, developmental process, immune system process, response to stimulation, cellular process, metabolic process, locomotion, biological adhesion, detoxification, and more. The enriched Molecular Function (MF) GO terms included binding, transporter activity, transcription regulator activity, molecular carrier activity, nutrient reservoir activity, and others. As for Cellular Component (CC) GO terms, they encompassed cell, organelle, protein-containing complex, extracellular region, and more (Fig. 2A).

Similarly, the up-regulated transcripts during the milking stage were found to be enriched in BP GO terms related to biological regulation, developmental process, metabolic process, localization, cellular component organization, locomotion, etc. The enriched MF GO terms included catalytic activity, binding, transporter activity, and transcription regulation activity, among others (Fig. 2B). Among the down-regulated transcripts, during both the spike emergence and milking stages, 111 and 272 transcripts respectively were enriched with GO terms related to various functions (Fig. 2C and D).

3.5. DEGs involved in transportation and uptakes of mineral

The intricate process of mineral uptake, transportation, and accumulation (including minerals like Zn, Fe, Cu, Ca, and Cd) from the roots to various parts of the plant is under the intricate control of a group of genes. In the context of the current barnyard millet

Table 4
Transcripts having dynamic association with Iron binding and metal-ion transfer during different stages of Barnyard Millet.

No	Protein family	Predicted Functions	#Up Regulated in Spike Stage	#Up Regulated in Milking stage
1	ABC Transporter family proteins	ATP binding; ATPase activity, coupled to transmembrane movement of substances	04	05
2	Calcium dependent kinase family	Calcium ion binding; F: protein binding	08	08
3	Ferritin	Primary intracellular iron-storage protein	01	00
4	metal ion binding	Metal ion binding activity	218	105
5	Iron-sulfur cluster binding	Iron-sulfur cluster binding	27	27
6	Cytochrome family	Iron ion binding; oxidoreductase activity, acting on paired donors, with incorporation or reduction of molecular oxygen,	26	08
7	Zinc finger transcription factor family	Transcription factor activity, sequence-specific DNA binding; metal ion binding; transcription regulatory region DNA,	08	06
8	Ferredoxin–NADP reductase type 1 family	Oxidoreductase activity, Ferredoxin reductase catalyzes the final step of electron transfer to make NADPH and ATP in plant chloroplasts during	03	02
9	Putative laccase Multicopper oxidase family	Ferroxidase activity; copper ion binding; plasma membrane; iron ion transport; lignin catabolic process	01	03
10	Terpene synthase family	Lyase activity; metal ion binding; magnesium ion binding	06	01

experiment, specific protein families responsible for mineral transportation and accumulation in different plant parts, originating from both roots and shoots, have been identified. These families encompass ABC Transporter proteins, Calcium-dependent kinase family, Ferritin, Metal ion binding proteins, Iron-sulfur cluster binding proteins, Cytochrome family, Zinc finger transcription factor family, Ferredoxin–NADP reductase type 1 family, Putative laccase, Multicopper oxidase family, and Terpene synthase family (Table 4). Notably, the number of up-regulated transcripts within the ABC transporter family was 4 and 5 during the spike emergence and milking stages, respectively. In the case of transcripts associated with the metal ion binding protein family, a significant up-regulation was observed during both stages, with 218 transcripts during spike emergence and 105 during the milking stage. This heightened presence suggests their vital role in metal ion binding activities. Additional protein families also displayed varying levels of up-regulation. For instance, the calcium-dependent kinase family showed 8 up-regulated transcripts during both the spike emergence and milking stages. The iron-sulfur cluster binding family had 27 up-regulated transcripts in each of these stages, cytochrome exhibited 26 in spike emergence and 8 in milking, Zinc finger transcription factor showed 8 in spike emergence and 6 in milking, Ferredoxin–NADP reductase type 1 family had 3 in spike emergence and 2 in milking, Putative laccase multi copper oxidase family revealed 1 in spike emergence and 3 in milking, and Terpene synthase presented 6 in spike emergence and 1 in milking.

Remarkably, the spike emergence stage demonstrated a higher number of up-regulated transcripts linked to mineral transportation and uptake families compared to the milking stage. This observation suggests that the spike emergence stage holds greater significance for mineral accumulation within the seeds as opposed to the subsequent stages. Consequently, during the spike emergence stage, it becomes crucial to provide the plant with an ample supply of minerals to facilitate their accumulation within the seeds. This strategic approach can contribute to enhancing mineral content in the final harvested produce.

3.6. Genes involved in high Fe uptake

The process of transporting iron (Fe) to various plant parts and its subsequent accumulation in grains is influenced by intrinsic genetic factors as well as external elements such as pH, water availability, and organic substances. Additionally, stress tolerance responses (STR) have been identified as contributing factors to the accumulation of both Fe and zinc (Zn) in grains and other plant parts, working alongside the genes directly involved in Fe and Zn accumulation.

In the current study, a closer examination of molecular functions related to binding revealed several significant aspects. These included cation binding, iron ion binding, metal cluster binding, organic cyclic compound binding, protein binding, small molecule binding, and zinc ion binding (Fig. 3). Interestingly, with the exception of carbohydrate binding, cation binding, chromatin binding, metal cluster binding, and organic cyclic compound binding, the molecular functions associated with ion binding were notably more pronounced during the spike emergence stage as opposed to the milking stage. This observation suggests that the spike emergence stage plays a particularly pivotal role in processes related to ion binding, especially when it comes to cation, iron ion, metal cluster, organic cyclic compound, protein, small molecule, and zinc ion binding. The prominence of these molecular functions during the spike emergence stage signifies its heightened importance in facilitating the intricate processes of Fe and Zn accumulation within the plant, further underscoring the significance of this stage in enhancing the nutritional content of grains and plant parts.

3.7. Metabolic process involved in uptakes of mineral transportation

Metabolic processes implicated in the uptake and transportation of minerals during both the spike emergence and milking stages of high iron (Fe) genotypes, utilizing KEGG pathway enrichment analysis were identified. Notably, during the spike emergence and milking stages, approximately 176 and 56 KEGG pathways respectively were found to exhibit enrichment among up-regulated transcripts. Our pathway analysis unveiled that certain pathways were significantly enriched during the spike emergence stage of high Fe barnyard millet genotypes. These pathways included Purine metabolism, Thiamine metabolism, Pyrimidine metabolism,
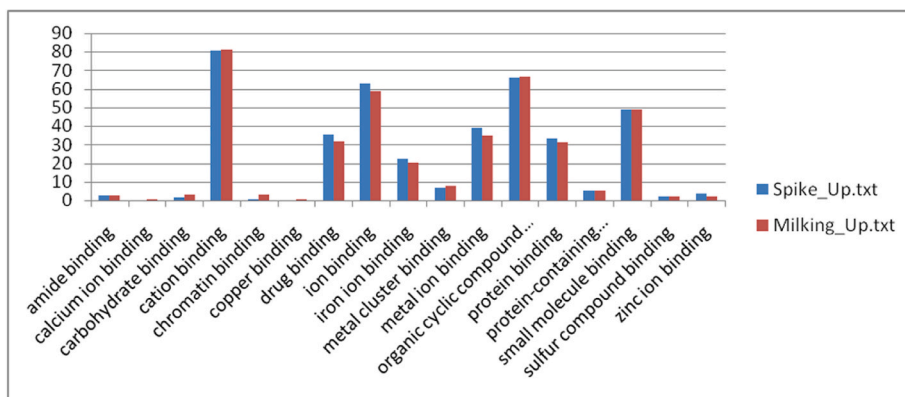

Fig. 3. Classification of ion binding component of molecular function which were up-regulated during the Spike and Milking stages of Barnyard Millet.

Arginine and proline metabolism, Drug metabolism - other enzymes, Tryptophan metabolism, Glycolysis/Gluconeogenesis, and phenylpropanoid biosynthesis. Among these, Purine metabolism, Thiamine metabolism, Pyrimidine metabolism, and Arginine and proline metabolism demonstrated particularly high levels of enrichment compared to other pathways. Furthermore, several pathways exhibited moderate enrichment during both developmental stages, including Pyruvate metabolism, Citrate cycle (TCA cycle), Aminoacyl-tRNA biosynthesis, Steroid hormone biosynthesis, and galactose metabolism.

Notably, the highly enriched enzymes encoded by the expressed genes during the spike emergence stage played vital roles in generating hydroxyl cinnamic acids, esters, guaiacyl, syringyl, and lignin. These pathways involved a range of enzymes, such as carboxykinase (GTP) (EC:4.1.1.32), dehydrogenase (NAD+) (EC:1.2.1.3), carboxykinase (ATP) (EC:4.1.1.49), 1-phosphotransferase (EC:2.7.1.90), acetyltransferase (EC:2.3.1.12), ligase (EC:6.2.1.1), kinase (EC:2.7.2.3), dehydrogenase (EC:1.8.1.4), dehydrogenase [NAD(P)+] (EC:1.2.1.5), synthase (EC:1.2.7.1), and glucokinase (phosphorylating) (EC:2.7.1.2). These biomolecules play pivotal roles and contribute indirectly to plant metabolic responses (Supplementary Fig. 4). The pathway enrichment analysis of differentially expressed genes (DEGs) related to the upregulation during the spike stage of high iron containing genotypes indicated the enrichment of pathways such as Zinc-dependent metalloprotease, Ferroxidase complex, ABC transporter family G domain, Flavonoid metabolic process, and Iron ion binding. Among these, Active transmembrane transporter activity featured 24 genes with a gene ratio of 0.03, while iron transport and ferroxidase complex were represented by 8 genes and 3 genes, respectively, with a gene ratio of 0.3. Additionally, other pathways involved in iron and metal transport are depicted in Fig. 4.

3.8. Gene co-expression analysis

The co-expression and physical network of all unregulated genes during the spike formation stage of the High Iron barnyard millet genotype are illustrated in Fig. 5A and B. Genes were identified using all available methods, and their interactions are depicted using colored lines. The black lines denote connections between these genes. Notably, certain proteins like TSC10, SDH2-3, BTS, ECA3, YSL8, AT5G48290, and NdHS exhibit strong co-expression and are critically involved in activities such as Metal ion transfer, Iron-sulfur metabolism, and mineral ion transport. These proteins collectively contribute to these important processes during the spike
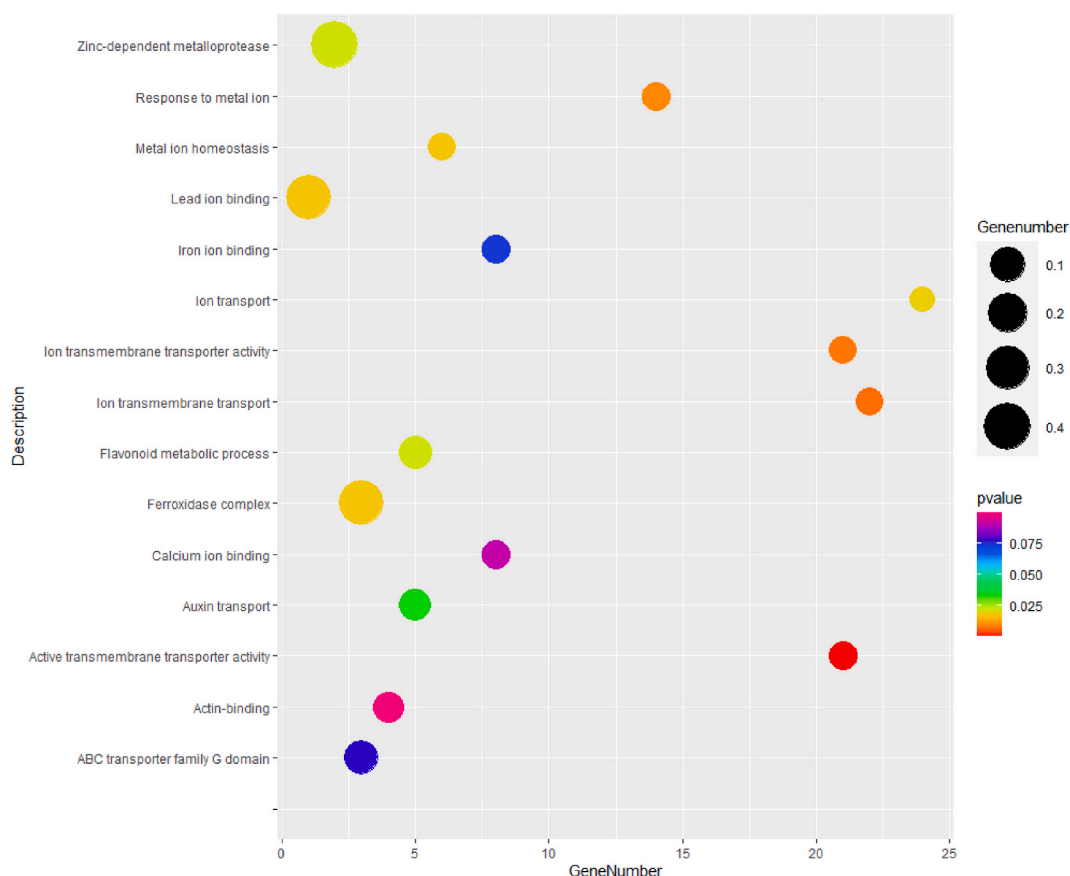

Fig. 4. Metal and iron uptake Pathway enrichment analysis of spike stage of high iron containing genotype. Each individual in the figure represents a pathway, the ordinate represents the name of the pathway, and the abscissa is the Gene Number, indicating the ratio of the gene proportion annotated to a pathway in the differential gene to that annotated to the pathway in all genes. The colour of the block represents p-value corrected by multiple hypothesis tests. (For interpretation of the references to colour in this figure legend, the reader is referred to the Web version of this article.)

formation stage. During the milking stage, specific proteins like PNsL4, FH (Frataxin), AT3412100, and YSL8 are engaged in metal ion transport. FH, also known as Frataxin protein, operates within the mitochondria and assumes a crucial role in facilitating heme biosynthesis, in addition to the assembly and repair of iron-sulfur clusters. This is achieved through the delivery of Fe (2+) to proteins participating in these pathways. Notably, FH also appears to play a role in safeguarding against iron-catalyzed oxidative stress. This network analysis provides valuable insights into the coordinated actions of these proteins, shedding light on their interplay and their pivotal roles in crucial biological processes related to metal ion transfer, iron-sulfur dynamics, mineral ion transport, and oxidative stress management.

3.9. Validation through qRT-PCR

A total of 6 contigs were selected, each representing a probable function related to metal transport, iron-sulfur dynamics, metal ion binding, auxin-responsive GH3-like protein 2, and cytochrome P450 71B16. These contigs were chosen for validation in both high and low iron (Fe) containing genotypes, during both spike emergence and milking stages (Table 5). Primers were designed based on these contigs and employed in quantitative real-time polymerase chain reaction (qRT-PCR) to validate their expression. The elongation factor (EF1) transcript was utilized as an endogenous control to normalize the relative gene expression of the targeted transcripts. Differential expression of these selected transcripts was observed in the context of both high and low Fe genotypes, as well as their
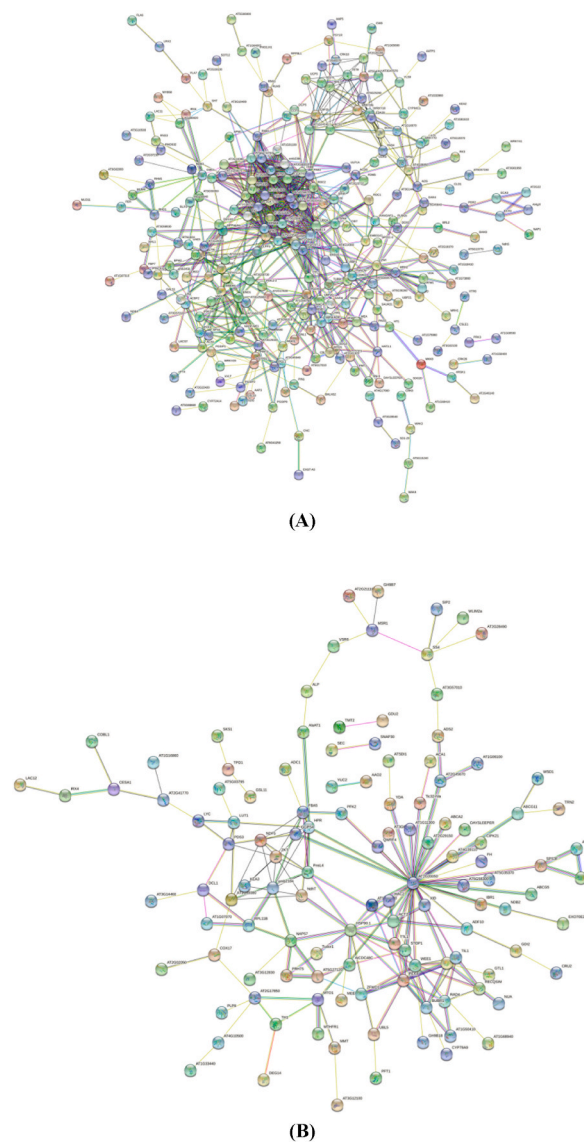
(A)

(B)

Fig. 5. Gene co-expression analyses of up-regulated genes in barnyard millet. (A) - Gene co-expression analyses of up-regulated genes in spike stage of barnyard millet; (B) - Gene co-expression analyses of up-regulated genes in milking stage of barnyard millet.

respective controls. Notably, the genes cbf5, gh32, and c71bg exhibited an up-regulated pattern during both stages of spike development. Conversely, gtl1 displayed down-regulation specifically during the spike emergence stage. The genes bon1 and tauE, on the other hand, showed an up-regulated pattern during the spike emergence stage and a down-regulated pattern during the milking stage (Fig. 6). Furthermore, transcripts associated with iron and metal uptake displayed an up-regulated trend during both developmental stages. However, the expression levels were notably higher during the spike emergence stage compared to the milking stage. Upon comparing the expression levels of these transcripts between transcriptome data and qRT-PCR results, a positive correlation was observed. While the fold change values did not exactly match, the consistent up-regulated and down-regulated expression patterns were maintained between the two methods. This validation process reinforces the reliability of the transcriptome data and provides confidence in the expression patterns observed in relation to the targeted genes involved in metal transport, iron-sulfur dynamics, and other crucial processes during the spike emergence and milking stages.

4. Discussion

Malnutrition remains a widespread concern on a global scale, prompting researchers worldwide to focus on addressing this issue. The development of cereal grains enriched with essential micronutrients represents a pivotal strategy to combat malnutrition. However, the capacity of genotypes to accumulate micronutrients, including iron (Fe), varies between different genotypes and developmental stages of grains. Transcriptome sequencing has been employed in previous studies on wheat and pearl millet to unravel the genetic components and transcripts associated with micronutrient accumulation in grains [13,29,30].

In the context of this study, our primary aim was to identify the specific genes responsible for Fe accumulation in barnyard millet grains. These genes encompass various protein families, such as ABC Transporter family proteins, Calcium-dependent kinase family, Ferritin, Metal ion binding proteins, Iron-sulfur cluster binding proteins, Cytochrome family, Zinc finger transcription factor family, Ferredoxin–NADP reductase type 1 family, Putative laccase, Multicopper oxidase family, and Terpene synthase [13,29,30]. Notably, the spike development stage emerged as a critical period for maximizing Fe accumulation in barnyard millet grains. A noteworthy discovery in this study was the enrichment of 27 iron-sulfur transcripts during both the spike emergence and milking stages of barnyard millet. These transcripts are indirectly associated with plant-type Ferredoxin (Fd), a small [2Fe–2S] cluster-containing protein renowned for its pivotal role in facilitating interactions with iron-sulfur proteins and various plant metabolites [31]. Importantly, only ferritin-related genes were expressed during the spike stage of high Fe-containing barnyard millet genotypes, aligning with earlier research that suggests ferritin's role in enabling Fe storage within the meristematic zone of *Arabidopsis thaliana* tissue architecture [32].

Several metabolic pathways, such as purine-pyrimidine metabolism, phenylpropanoid biosynthesis, and terpene synthase, demonstrated putative enrichment in elite barnyard millet genotypes. These pathways have been reported in other plants as responsive to stress-related pathways [33], highlighting the complex regulatory mechanisms plants employ to manage environmental challenges. Significantly, the presence of multiple differentially expressed genes (DEGs) and co-factors related to Fe and ion transport proteins suggests their integral roles in orchestrating the regulation of key genes involved in these processes.

Our findings unequivocally emphasize that the spike emergence stage holds paramount importance for micronutrient accumulation in barnyard millet grains. This implies that optimal soil enrichment for higher micronutrient accumulation should occur precisely during spike emergence, rather than waiting until after the spike has fully developed. The application of micronutrients to the soil at the spike emergence stage stands to maximize Fe and other micronutrient accumulation in grains. This strategy is grounded in the active involvement of numerous transcripts responsible for micronutrient accumulation during the spike emergence stage, in contrast to the milking stage. These outcomes provide valuable insights for breeders aiming to enhance Fe and micronutrient accumulation in barnyard millet genotypes, as well as for agronomists seeking effective soil nutrient management strategies to elevate micronutrient content in grains.

This investigation not only contributes to our understanding of micronutrient accumulation in barnyard millet but also provides actionable insights that can potentially address malnutrition and contribute to enhanced agricultural practices. By shedding light on the critical role of specific developmental stages and genetic factors, this study paves the way for targeted interventions to boost the nutritional quality of crops and ultimately improve human health.

5. Conclusions

Barnyard millet is a climate-resilient cereal crop with high nutritive value, possessing the potential to supply the essential iron (Fe) content needed for daily dietary requirements. It exhibits significant genetic diversity in grain Fe content across different genotypes. Our transcriptome sequencing results, encompassing two key stages of spike development in barnyard millet genotypes with varying Fe content, have unveiled a crucial revelation: the spike emergence stage holds greater importance for Fe accumulation compared to the milking stage. Supplying Fe and other micronutrients to plants during the spike emergence stage leads to a more pronounced accumulation of Fe and other vital nutrients in the grains compared to other spike development stages. The protein families identified, including ABC Transporter family proteins, Calcium-dependent kinase family, Ferritin, Metal ion binding proteins, Iron-sulfur cluster binding proteins, Cytochrome family, Zinc finger transcription factor family, Ferredoxin–NADP reductase type 1 family, Putative laccase, Multicopper oxidase family, and Terpene synthase family, may play significant roles in Fe accumulation within the grains. These Ferritin and Iron-sulfur cluster binding genes, along with other candidate genes, warrant comprehensive investigation across diverse barnyard germplasm to elucidate their roles further. These genetic elements hold potential as key contributors to Fe accumulation mechanisms. The transcriptome data generated in this study offers a foundation for the development of breeder-friendly

Table 5
List of primers used for the validation through qRT PCR.

Contig No.	Probable function	name		Primer seq	Product size
Contig3088.p1	Metal transporter	cbf5	F	AGTTAGACCACTCGAAGGCA	200
			R	TTGTCATCAACGCAACACCT	
Contig16455.p2	Iron sulfur	gtl1	F	GTCGGCGCCTATAGATCTCC	201
			R	GTGGTCGTCAAGTATCCCGA	
Contig2221.p1	Metal ion binding	bon1	F	GCAAGCAGTACGTCCAGAAG	168
			R	ACTGGTGGGTGACGTAGAAC	
Contig3220.p1	Metal ion binding	tauE	F	TTGCCTGAAACCTCAACAGC	155
			R	AGGTGGACGTAGCACTTGAA	
Contig19585.p1	Auxin-responsive GH3-like protein 2	gh32	F	CCATCAACCAGTACAAGGCG	154
			R	TCCACCGTACCGAATTCCAT	
Contig21556.p2	Cytochrome P450 71B16	c71bg	F	CCCTCCACTATCACCACCAA	160
			R	GTCATACGCCGGACCAAAC	
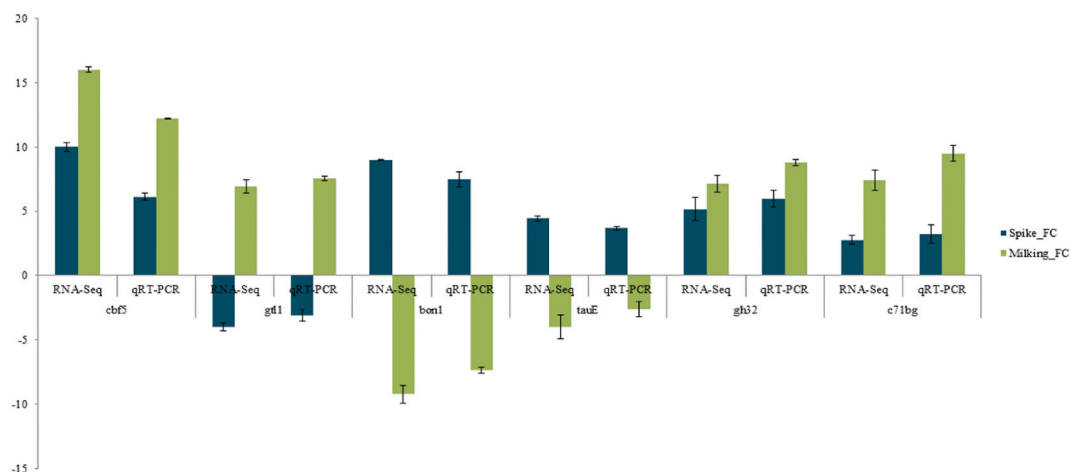
Fig. 6. qRT PCR validation of transcripts.

marker systems, aimed at enhancing grain Fe content in barnyard millet. These marker systems can facilitate the advancement of millet breeding programs, culminating in improved crop varieties with heightened nutritional value. Our findings also sheds light on Fe accumulation dynamics and genetic players, and promise to underpin strategies that elevate barnyard millet's role in fortifying diets and bolstering global food security.

Data availability statement

All the data presented in the manuscript are publicly available in NCBI with Bio-project Number PRJNA748838 and Sample Accession number SAMN20354950- SAMN20354979. Some of the gene expression data generated during this study are available as a supplementary file while the rest of the data can be availed from the corresponding author(s) on request. All authors have read and accepted the MS.

Ethics statement

Review and/or approval by an ethics committee and informed consent was not required for this study, as no participants not involved in the preparation of the manuscript were required for the experiments performed.

CRediT authorship contribution statement

Shital M. Padhiyar: Investigation. **Jasminkumar Kheni:** Data curation. **Shraddha B. Bhatt:** Supervision, Formal analysis. **Hiral Desai:** Formal analysis. **Rukam S. Tomar:** Writing – review & editing, Conceptualization.

Declaration of competing interest

The authors declare that they have no known competing financial interests or personal relationships that could have appeared to influence the work reported in this paper.

Acknowledgments

Appendix A. Supplementary data

Supplementary data to this article can be found online at https://doi.org/10.1016/j.heliyon.2024.e30925.

References

[1] S. Perumal, M. Jayakodi, D.S. Kim, T.J. Yang, S. Natesan, The complete chloroplast genome sequence of Indian barnyard millet, Echinochloa frumentacea (Poaceae), Mitochondrial DNA Part B 1 (2016) 79–80, https://doi.org/10.1080/23802359.2015.1137832.
[2] S.S. Gomashe, Barnyard Millet: Present Status and Future Thrust Areas in Millets and Sorghum: Biology and Genetic Improvement, John Wiley & Sons, Hoboken, NJ, USA, 2016, pp. 184–198, https://doi.org/10.1002/9781119130765.ch7.
[3] IIMR, Annual Report 2017-18, Indian Institute of Millets Research, Hyderabad, 2018.
[4] S. Sood, R.K. Khulbe, A.K. Gupta, P.K. Agrawal, H.D. Upadhyaya, J.C. Bhatt, Barnyard millet - a potential food and feed crop of future, Plant Breed. 134 (2015) 135–147, https://doi.org/10.1111/pbr.12243.
[5] R. Ugare, B. Chimmad, R. Naik, P. Bharati, S. Itagi, Glycemic index and significance of barnyard millet (*Echinochloa frumentacae*) in type II diabetics, J. Food Sci. Technol. 51 (2) (2014) 392–395, https://doi.org/10.1007/s13197-011-0516-8.
[6] S.K. Kumari, B. Thayumanavan, Comparative study of resistant starch from minor millets on intestinal responses, blood glucose, serum cholesterol and triglycerides in rats, J. Food Sci. Technol. 75 (1997) 296–302.
[7] World Health Organization, Micronutrients, 2023. https://www.who.int/health-topics/micronutrients. June 2023.
[8] T. Longvah, R. Ananthan, K. Bhaskarachary, K. Venkaiah, Indian Food Composition Table, National Institute of Nutrition, Hyderabad, 2017, pp. 1–578.
[9] R.S. Tomar, Molecular Markers and Plant Biotechnology, New India Publishing, New Delhi, 2010.
[10] R.S. Annadurai, V.M. Jayakumar, R.C. Mugasimangalam, Next generation sequencing and de novo transcriptome analysis of Costus pictus D. Don, a non-model plant with potent anti-diabetic properties, BMC Genom. 13 (2012) 663–672, https://doi.org/10.1186/1471-2164-13-663.
[11] J. Lu, Z.X. Du, J. Kong, L.N. Chen, Y.H. Qiu, G.F. Li, X.H. Meng, S.F. Zhu, Transcriptome analysis of Nicotiana tabacum infected by Cucumber mosaic virus during systemic symptom development, PLoS One 7 (8) (2012) e43447, https://doi.org/10.1371/journal.pone.0043447.
[12] S. Jaiswal, P.V. Jadhav, R.S. Jasrotia, P.B. Kale, S.K. Kad, M.P. Moharil, M.S. Dudhare, J. Kheni, A.G. Deshmukh, S.S. Mane, R.S. Nandanwar, S. Penna, J. G. Manjaya, A.M. Iquebal, R.S. Tomar, P.G. Kawar, A. Rai, Kumar Dinesh, Transcriptomic signature reveals mechanism of flower bud distortion in witches'-broom disease of soybean (Glycine max), BMC Plant Biol. 19 (26) (2019) 1–12, https://doi.org/10.1186/s12870-018-1601-1.
[13] C.T. Satyavathi, R.S. Tomar, S. Ambawat, J. Kheni, S.M. Padhiyar, H. Desai, S.B. Bhatt, M.S. Shitap, R.C. Meena, T. Singhal, S.M. Sankar, S.P. Singh, V. Khandelwal, Stage specific comparative transcriptomic analysis to reveal gene networks regulating iron and zinc content in pearl millet [Pennisetum glaucum (L.) R. Br.], Sci. Rep. 12 (276) (2022) 1–13, https://doi.org/10.1038/s41598-021-04388-0.
[14] J.H. Strickler, A.N. Starodub, J. Jia, K.L. Meadows, A.B. Nixon, A. Dellinger, M.A. Morse, H.E. Uronis, P.K. Marcom, S.Y. Zafar, S.T. Haley, H.I. Hurwitz, Phase I study of bevacizumab, everolimus, and panobinostat (LBH-589) in advanced solid tumors, Cancer Chemother. Pharmacol. 70 (2) (2012) 251–258, https://doi. org/10.1007/s00280-012-1911-1.
[15] K.S. Arun-Chinnappa, D.W. McCurdy, De novo assembly of a genome-wide transcriptome map of Vicia faba (L.) for transfer cell research, Front. Plant Sci. 6 (217) (2015) 1–9, https://doi.org/10.3389/fpls.2015.00217.
[16] S. Andrews, FastQC, 2015. https://qubeshub.org/resources/fastqc.
[17] M.G. Grabherr, B.J. Haas, M. Yassour, J.Z. Levin, D.A. Thompson, I. Amit, X. Adiconis, L. Fan, R. Raychowdhury, Q. Zeng, Z. Chen, E. Mauceli, N. Hacohen, A. Gnirke, N. Rhind, F. Palma, B.W. Birren, C. Nusbaum, K. Lindblad-Toh, N. Friedman, A. Regev, Full-length transcriptome assembly from RNA-Seq data without a reference genome, Nat. Biotechnol. 29 (2011) 644–652, https://doi.org/10.1038/nbt.1883.
[18] B. Haas, A. Papanicolaou, M. Yassour, M. Grabherr, P.D. Blood, J. Bowden, M.B. Couger, D. Eccles, B. Li, M. Lieber, M.D. MacManes, M. Ott, J. Orvis, N. Pochet, F. Strozzi, N. Weeks, R. Westerman, T. William, C.N. Dewey, R. Henschel, R.D. LeDuc, N. Friedman, A. Regev, De novo transcript sequence reconstruction from RNA-seq using the Trinity platform for reference generation and analysis, Nat. Protoc. 8 (2013) 1494–1512, https://doi.org/10.1038/nprot.2013.084.
[19] X. Huang, A. Madan, CAP3: a DNA sequence assembly program, Genome Res. 9 (9) (1999) 868–877, https://doi.org/10.1101/gr.9.9.868.
[20] L. Fu, B. Niu, Z. Zhu, S. Wu, W. Li, CD-HIT: accelerated for clustering the next-generation sequencing data, Bioinformation 28 (23) (2012) 3150–3152, https:// doi.org/10.1093/bioinformatics/bts565.
[21] B. Langmead, S. Salzberg, Fast gapped-read alignment with Bowtie 2, Nat. Methods 9 (2012) 357–359, https://doi.org/10.1038/nmeth.1923.
[22] M.D. Robinson, D.J. McCarthy, G.K. Smyth, edgeR: a Bioconductor package for differential expression analysis of digital gene expression data, Bioinformation 26 (1) (2010) 139–140, https://doi.org/10.1093/bioinformatics/btp616.
[23] S.F. Altschul, W. Gish, W. Miller, E.W. Myers, D.J. Lipman, Basic local alignment search tool, J. Mol. Biol. 215 (1990) 403–410, https://doi.org/10.1016/S0022-2836(05)80360-2.
[24] C. Camacho, G. Coulouris, V. Avagyan, N. Ma, J. Papadopoulos, K. Bealer, T.L. Madden, BLAST+: architecture and applications, BMC Bioinf. 10 (421) (2009) 1–9, https://doi.org/10.1186/1471-2105-10-421.
[25] B. Usadel, F. Poree, A. Nagel, M. Lohse, A. Czedik-Eysenberg, M. Stitt, A guide to using MapMan to visualize and compare Omics data in plants: a case study in the crop species, Maize, Plant Cell Environ. 9 (2009) 1211–1229, https://doi.org/10.1111/j.1365-3040.2009.
[26] S.X. Ge, D. Jung, R. Yao, A graphical gene-set enrichment tool for animals and plants, Bioinformation 36 (8) (2020) 2628–2629, https://doi.org/10.1093/ bioinformatics/btz931.
[27] T. Thiel, MISA-Microsatellite identification tool. http://pgrc.ipk-gatersleben.de/misa/, 2003.
[28] K.J. Livak, T.D. Schmittgen, Analysis of relative gene expression data using real-time quantitative PCR and the 2− ∆∆CT method, Methods 25 (4) (2001) 402–408, https://doi.org/10.1006/meth.2001.1262.

[29] S. Shi, S. Li, M. Asim, J. Mao, D. Xu, Z. Ullah, G. Liu, Q. Wang, H. Liu, The Arabidopsis Calcium-Dependent Protein Kinases (CDPKs) and their roles in plant growth regulation and abiotic stress responses, Int. J. Mol. Sci. 19 (7) (2018) 1900, https://doi.org/10.3390/ijms19071900.

[30] R. Wimalasekera, G.F. Scherer, Involvement of mitogen-activated protein kinases in abiotic stress responses in plants, Plant Metabolites and Regulation Under Environmental Stress (2018) 389–395, https://doi.org/10.4161/psb.6.2.14701.

[31] G. Hanke, P. Mulo, Plant type ferredoxins and ferredoxin-dependent metabolism, Plant Cell Environ. 36 (6) (2013) 1071–1084, https://doi.org/10.1111/pce.12046.

[32] G. Reyt, S. Boudouf, J. Boucherez, F. Gaymard, F. Briat, Iron- and ferritin-dependent reactive Oxygen species distribution: impact on Arabidopsis root system architecture, Mol. Plant 8 (3) (2015) 439–453, https://doi.org/10.1016/j.molp.2014.11.014.

[33] T. Vogt, Phenylpropanoid biosynthesis, Mol. Plant 3 (1) (2010) 2–20, https://doi.org/10.1093/mp/ssp106.